ROYAL SOCIETY OF CHEMISTRY

REVIEW

Check for updates

Developing better ester- and ether-based electrolytes for potassium-ion batteries†

Lin Li, [a] Shuo Zhao, [a] Zhe Hu, [b] Shu-Lei Chou [*ab] and Jun Chen [a]

Potassium-ion batteries (PIBs) have attracted extensive attention for next-generation energy storage systems because of the high abundance of potassium resources and low cost. However, the electrochemical performance of PIBs still cannot satisfy the requirements of practical application. One of the most effective strategies to improve the electrochemical performance of PIBs is electrolyte optimization. In this review, we focus on recent advances in ester- and ether-based electrolytes for high-performance PIBs. First, we discuss the requirements and components of organic electrolytes (potassium salts and solvents) for PIBs. Then, the strategies toward optimizing the electrolytes have been summarized, including potassium salt optimization, solvent optimization, electrolyte concentration optimization, and introducing electrolyte additives. In general, the electrolyte optimization methods can adjust the solvation energy, the lowest unoccupied molecular orbital energy level, and the highest occupied molecular orbital energy level, which are beneficial for achieving fast kinetics, stable and highly K^+-conductive solid-electrolyte interphase layer, and superior oxidation resistance, respectively. Future studies should focus on exploring the effects of composition on electrolyte characteristics and the corresponding laws. This review provides some significant guidance to develop better electrolytes for high-performance PIBs.

1   Introduction

With the rapid increase of energy consumption in the modern society, sustainable energy resources such as solar, wind and geothermal resources have attracted wide attention in recent years.[1–5] However, these sustainable energy resources are inherently intermittent and generally dispersed.[6,7] Thus, developing advanced large-scale energy storage technologies (mechanical, electrical, chemical and electrochemical) for sustainable energy is very important. Among these energy storage technologies, electrochemical energy storage technology has attracted extensive attention because of the long cycle life, low maintenance and pollution-free operation.[8,9] In the past decades, lithium-ion batteries (LIBs) have been successfully applied for portable electronic devices and electric vehicles owing to the high energy density and superior cycling stability.[10–13] Nevertheless, the application of LIBs for large-scale energy storage systems is hindered by the limited Li resources and relatively high cost.[14,15]

Recently, more and more researchers have focused on developing new battery systems based on more abundant

elements such as sodium, potassium, magnesium, calcium, zinc, and aluminum.[11,16] Among these new battery systems, potassium ion batteries (PIBs) with the "rocking-chair" working mechanism have attracted extensive attention because the potassium metal anode shows the lowest standard redox potential (−2.93 V *versus* standard hydrogen electrode).[17–19] In addition, potassium does not react with aluminum.[20] Thus, aluminum can replace copper as the anode current collector, reducing the whole cost of PIBs. The potassium metal anode exhibits theoretical gravimetric and volumetric capacities of 685 mA h g^{-1} and 609 mA h cm^{-3}, respectively.[15] The interactions between K^+ and organic solvents are relatively weak due to the large ionic radius and weak Lewis acidity of K.[21] The weak interactions are beneficial for PIBs to achieve high rate performance. More importantly, the crustal abundance of potassium (1.5 wt%) is much higher than that of lithium (0.0017 wt%).[22,23] Therefore, PIBs are one of the most promising potential candidates for large-scale energy storage systems.

In general, PIBs mainly consist of a cathode, a separator, an electrolyte and an anode (Fig. 1a). The cathode and anode materials can reversibly store K^+ ions. The separator and electrolyte are applied to avoid short circuit of the battery and promote ion transfer, respectively. During the charging process, K^+ deintercalates from the cathode (*e.g.*, layered materials,[24] Prussian blue analogues,[25] organic materials,[26] and polyanionic compounds[27]) and then gets inserted into the anode (*e.g.*, carbon materials,[28] organic materials,[29] metals[30] and metal oxides[31]). In the subsequent discharging process, K^+

aKey Laboratory of Advanced Energy Materials Chemistry (Ministry of Education), Renewable Energy Conversion and Storage Center, College of Chemistry, Nankai University, Tianjin 300071, China. E-mail: shulei@uow.edu.au

bInstitute for Superconducting and Electronic Materials Australian Institute for Innovative Materials, University of Wollongong, Innovation Campus, Wollongong, New South Wales 2522, Australia

† Dedicated to the 100th anniversary of Chemistry at Nankai University.
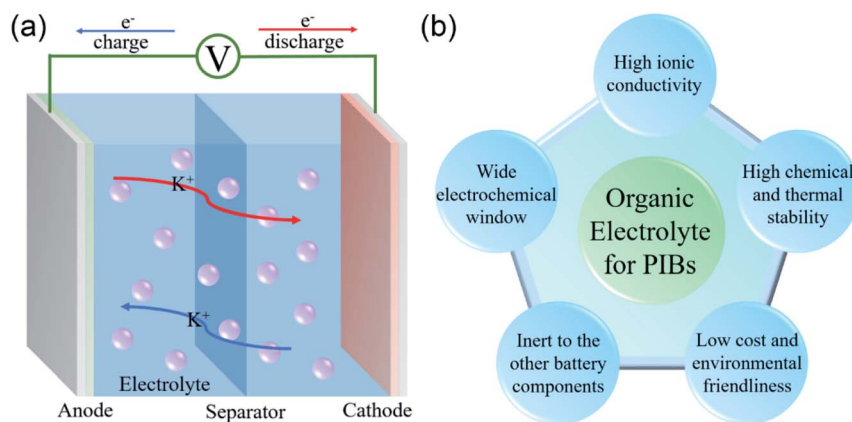
Fig. 1 (a) Schematic operation principle of PIBs. (b) The requirements of organic electrolytes for PIBs.

deintercalates from the anode and then gets inserted into the cathode. The whole reaction process is highly reversible.

The electrolyte is a key component and plays an important role in ion transfer between the electrodes in PIBs. The electrochemical stability window of the electrolyte determines the available electrode materials, and thus affects the energy density of PIBs.[32] In addition, the properties (such as the lowest unoccupied molecular orbital, LUMO) of the electrolyte are closely related to the formation of the solid-electrolyte interphase (SEI) layer on the anode, which significantly affects the electrochemical performance of batteries.[12,33,34] However, until now, it has been challenging to develop a suitable electrolyte with both a wide electrochemical stability window and a stable interface toward the anode (by forming a stable SEI layer). Therefore, optimizing the electrolyte is important for developing high-performance PIBs. In general, the electrolyte for PIBs can be grouped into three categories: liquid, quasi-solid-state, and all-solid-state electrolytes.[17,26,35–37] Among these types of electrolytes, organic electrolytes based on esters and ethers are the most extensively applied electrolytes in PIBs. In general, ester-based electrolytes show good oxidation resistance and can match with high-voltage cathodes. Compared with ester-based electrolytes, ether-based electrolytes exhibit lower oxidation voltage but tend to form a thinner SEI layer, which is beneficial for improving the kinetics. Until now, to the best of our knowledge, less attention has been paid to summarize organic electrolyte optimization for PIBs. Thus, a comprehensive summary on how to optimize ester- and ether-based electrolytes for high-performance PIBs is very significant.

In this review, we focus on the recent research progress in organic electrolytes based on esters and ethers for PIBs. We first introduce the requirements and basic compositions (potassium salts and solvents) of organic electrolytes for PIBs. Then, we summarize the optimization strategies of organic electrolytes for PIBs, including potassium salt optimization, solvent optimization, electrolyte concentration optimization, and introducing electrolyte additives. Finally, future perspectives on organic electrolytes for PIBs are also proposed.

2 Requirements and components of organic electrolytes for PIBs

2.1 Requirements of organic electrolytes for PIBs

Organic electrolytes based on ester and ether solvents are the most widely used electrolyte systems in PIBs. In general, the organic electrolyte for PIBs consists of potassium salts and organic solvents. Theoretically, the organic electrolyte candidates for PIBs should satisfy the following requirements (Fig. 1b):[38,39] (i) high ionic conductivity; (ii) wide electrochemical window, (iii) high chemical and thermal stability; (iv) inertness towards other battery components (current collectors, electrodes and separator); (v) low cost and environmental friendliness.

2.2 Components of organic electrolytes for PIBs

2.2.1 Potassium salts. Potassium salts play a key role in an organic electrolyte, which is an important factor dominating the performance of the organic electrolyte. In general, the ideal potassium salts for potassium-ion battery electrolytes should meet the following prerequisites:[39] (i) low dissociation energy and high solubility; (ii) good chemical, thermal and electrochemical stability; (iii) inertness towards the other battery components; (iv) helps to form a uniform and stable SEI layer; (v) low cost and environmental friendliness.

Only a few potassium salts can simultaneously meet the above requirements. Table 1 shows the basic physical properties of commonly used potassium salts for electrolytes in PIBs. Among these potassium salts, KPF_6 is the most widely studied salt in PIBs. However, the P–F bonds easily undergo hydrolysis to produce the highly corrosive HF.[39] Potassium bis(fluorosulfonyl)imide (KFSI) and potassium bis(trifluoromethanesulfonyl)imide (KTFSI) are extensively applied in high-concentration electrolytes (HCEs) because of their high solubility in commonly used ester and ether solvents in PIBs.[40] In addition, KFSI forms a uniform and stable solid electrolyte interphase layer.[41] The major drawback of KTFSI and KFSI is the corrosion of the anions toward the aluminum collector. Except for these three salts, some other potassium salts such as $KClO_4$ and KCF_3SO_3 have also been applied in PIBs.

Table 1 The commonly used potassium salts for electrolytes in PIBs

Salt	Structure	M. wt	T_m/°C	Al-corrosion
KPF_6		184.1	575	No
KFSI		219.2	102	Yes
KTFSI		319.2	∼200	Yes
$KClO_4$		138.5	610	No
KCF_3SO_3		188.2	238.5	Yes

2.2.2 Solvent. Solvent is another important part of the organic electrolyte. The ideal solvents for potassium-ion battery electrolytes should meet the following requirements:[39] (i) high dielectric constant; (ii) low viscosity and volatility; (iii) good stability (including chemical, thermal and electrochemical stability); (iv) inertness towards the other battery components; (v) low melting point, high boiling point; (vi) low cost and environmental friendliness. In this review, we focus on ester and ether solvents.

Esters have been extensively applied as solvents for commercial LIBs, and they are also adopted as solvents for PIBs. In general, the ester solvents for PIBs can be divided into two categories: cyclic carbonates (ethylene carbonate (EC) and propylene carbonate (PC)) and linear carbonates (diethyl carbonate (DEC), ethyl methyl carbonate (EMC) and dimethyl carbonate (DMC)). Cyclic carbonates (EC and PC) show huge potential for PIBs because of their high dielectric constant. Linear carbonates (DEC, EMC and DMC) are frequently applied as cosolvents with cyclic carbonates (EC or PC) to obtain an electrolyte with desirable performance. Most of the ester-based electrolytes for PIBs are composed of binary or ternary carbonate ester solvents. Recently, ether solvents have attracted extensive attention as some reported electrodes for PIBs show good stability in ether-based electrolytes.[42–44] Linear ethers (dimethoxyethane (DME), diethylene glycol dimethyl ether (DEGDME) and tetraethylene glycol dimethyl ether (TEGDME)) are the most commonly used ether solvents in PIBs. They show similar dielectric constants. DME and DEGDME are more attractive solvents for PIBs than TEGDME due to the relatively low viscosity. But TEGDME with a relatively high boiling point exhibits low volatility. The basic physical properties of the commonly used ester and ether solvents for PIB electrolytes have been summarized in Table 2.[39,45]

3 Electrolyte optimization

An organic electrolyte is an important factor affecting the electrochemical performance of PIBs. Recently, more and more groups have focused on optimizing the electrolyte to improve the electrochemical performance of electrode materials in PIBs.[24,46,47] Until now, the reported strategies to optimize the electrolyte in PIBs can be grouped into four categories: (i) potassium salt optimization;[48] (ii) solvent optimization;[49] (iii) electrolyte concentration optimization;[50] (iv) introducing electrolyte additives.[51]

Table 2 Physical properties of the commonly used ester and ether solvents for electrolytes in PIBs

Solvent	Structure	ε/(25 °C)	η/(cP, 25 °C)	T_m/°C	T_b/°C	d/(g cm^{-3}, 25 °C)
EC		89.78	1.9, 40 °C	36.4	248	1.321
PC		64.92	2.53	−48.8	242	1.200
DEC		2.805	0.75	−74.3	126	0.969
EMC		2.958	0.65	−53	110	1.006
DMC		3.107	0.59, 20 °C	4.6	91	1.063
DME		7.2	0.46	−58	84	0.86
DEGDME		7.3	0.99	−68	162	0.944
TEGDME		7.9	4.05	−30	275	1.009

3.1 Potassium salt optimization

It's well known that the electrochemical performance of electrolytes is related to the types of salts in the electrolyte.[52,53] To understand the effect of potassium salts in PIBs, Wu's group investigated the reversibility of K plating/stripping in various electrolytes (KFSI–DME, KTFSI–DME, KPF_6–DME and KPF_6–EC/DEC electrolyte).[53] The K/Cu half-cell shows high stability in the long term (100 cycles) in the KFSI–DME electrolyte. The other types of electrolytes all show poor electrochemical performance. Moreover, they found that the electrochemically plated K metal in KFSI–DME electrolyte exhibited a flat and uniform morphology. They proposed that the superior stability of the K/Cu half-cell and the ordered surface morphology of K metal in the KFSI-based electrolyte could be beneficial for the cooperative functioning of the organic and inorganic components of the SEI. However, the influence of potassium salts on SEI formation is not clear.

Recently, Guo *et al.* also demonstrated that optimizing the potassium salts can effectively improve the electrochemical performance of K metal.[54] Raman spectroscopy was used to investigate the interaction between electrolyte salts and solvents in electrolytes (Fig. 2a). The results reveal that KFSI shows stronger solvation than KPF_6. The stronger solvation will lower the amount of free solvent in the electrolyte, which is helpful for reducing the side reactions between K metal and solvent molecules. Thus, the symmetric K cells with the KFSI-based electrolyte show better electrochemical performance than that with the KPF_6-based electrolyte.

In addition, the red phosphorus/carbon nanotube@reduced graphene oxide (RP/C) anode also shows good cycling stability in the KFSI-based carbonate electrolyte. To understand the superior electrochemical performance of the RP/C anode in the KFSI-based carbonate electrolyte, the composition of SEI layers on the surface of the RP/C anode was investigated by X-ray photoelectron spectroscopy (XPS). Compared to the SEI layer in the KPF_6-based carbonate electrolyte, more inorganic salts were produced in the KFSI-based carbonate electrolyte (Fig. 2b). The stable and KF-rich organic–inorganic SEI layers are beneficial for accommodating the volume change of electrodes. The reason for the stable SEI formation in the KFSI-based carbonate electrolyte was also investigated by density functional theory calculations. Compared with the KPF_6-based electrolyte, the KFSI-based electrolyte showed higher solvation energy (Fig. 2c). There was relatively less free solvent in the KFSI-based electrolyte, which is beneficial for reducing side reactions. Besides, the KFSI–EC/DEC-based electrolyte shows lower solvation energy than the KFSI–DME electrolyte, indicating a relatively weak interaction between the solvent and potassium. The low solvation energy facilitates K^+ desolvation and diffusion, and then improves the kinetics. Fig. 2d shows the molecular energy levels of the highest occupied molecular orbital (HOMO) and the LUMO of salt–solvent complexes and solvation K^+ ions in various electrolytes. The LUMO energy level of KFSI–EC/DEC is lower than that of KPF_6–EC/DEC. The result indicates that the decomposition of KFSI occurs prior to that of KPF_6. These results demonstrate that the KFSI-based carbonate electrolyte favors the formation of stable and KF-rich organic–inorganic SEI layers on the surface of the electrode. Nevertheless, this work only investigated the effect of the electrolyte in half cells, it is not clear whether salt selection affects the working electrodes or K metal itself. Therefore, it's necessary to investigate the electrolyte in full cells.

In addition to K metal and RP/C anodes, the electrochemical performance of several anode materials (including Bi, Sn, Sb, Sn_4P_3, GeP_5 and MoS_2, *etc.*) is also affected by the potassium salts.[41,46,55–58] Based on previous investigations of potassium salts in PIBs, the potassium salts play an important role in the SEI layer formation. A stable SEI layer is beneficial for improving the electrochemical performance of electrode materials. Therefore, it is significant to carefully design novel potassium salts to build a stable SEI layer on the surface of the electrode for high-performance PIBs.
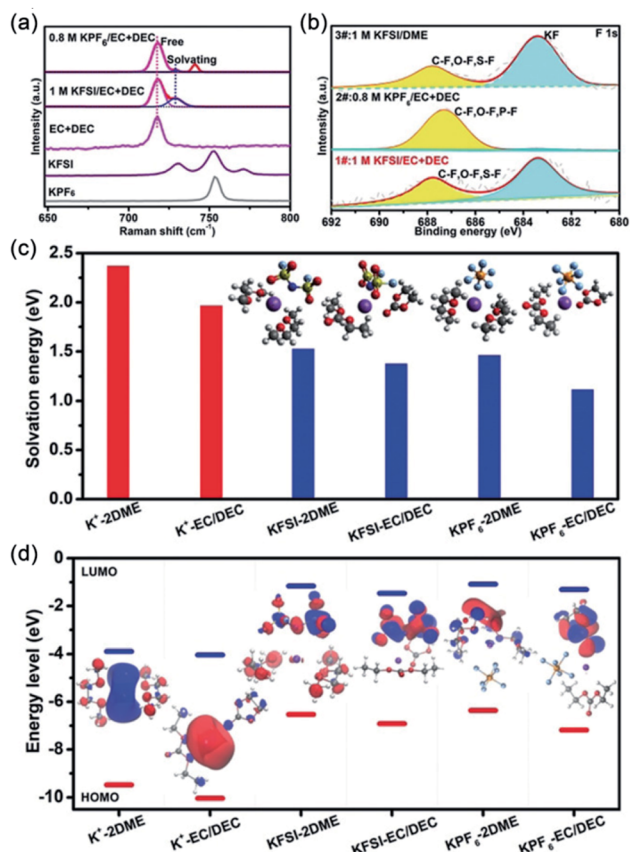

Fig. 2 (a) Raman spectra of ester-based electrolytes. (b) F1s XPS spectra of discharged RP/C anodes after 10 cycles in different types of electrolytes. (c) Solvation energies and (d) LUMO–HOMO energy levels of salt–solvent complexes and solvation K^+ ions in various electrolytes. (a–d) Reproduced with permission.[54] Copyright 2019, Wiley-VCH.

3.2 Solvent optimization

Different types of electrolyte solvents will also affect the electrochemical performance of electrode materials in PIBs.[59–62] In 2016, Xu's group tested the electrochemical performance of graphite anodes in different electrolyte solvents (EC:PC,
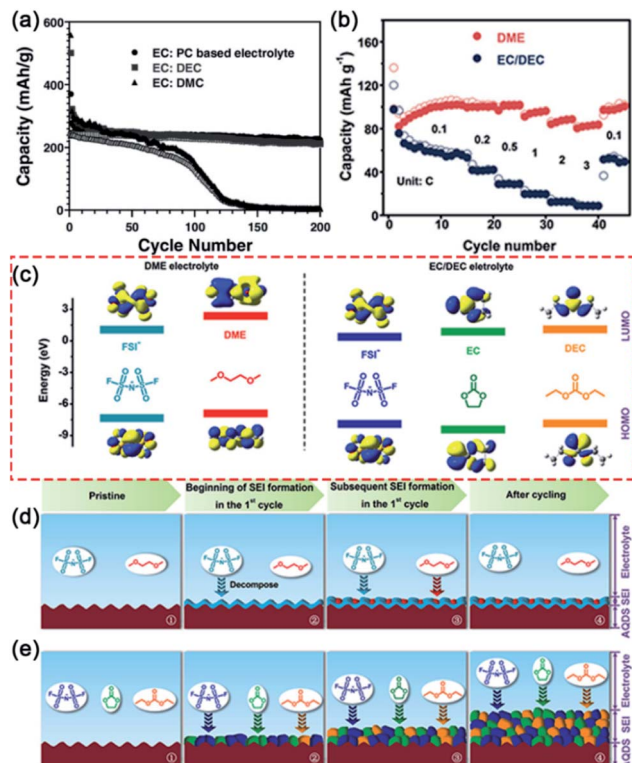
Fig. 3 (a) Cycling performance of the graphite electrode in different electrolytes. Reproduced with permission.[59] Copyright 2016, Wiley-VCH. (b) Rate performance of AQDS electrodes in different electrolytes. (c) The HOMO and LUMO energy levels of solvents and potassium salts in different electrolytes. Schematic illustration of the SEI formation in (d) 0.8 M KFSI DME electrolyte and (e) 0.8 M KFSI EC/DEC electrolyte. (b–e) Reproduced with permission.[68] Copyright 2018, Wiley-VCH.

EC:DEC and EC:DMC) with KPF_6 salt.[59] As shown in Fig. 3a, the graphite anode in KPF_6–EC:PC electrolyte shows superior cycling stability and high coulombic efficiency. They proposed that the inferior electrochemical performance of KPF_6–EC:DEC and KPF_6–EC:DMC electrolyte results from the more stable SEI layer formed in KPF_6–EC:PC. Moreover, Guo and co-workers investigated the effect of different solvents (DMC, DEC and EC/DEC) on the electrochemical performance of the $SnSb_2Te_4$/G anode in PIBs.[62] Compared with KFSI–DEC and KFSI–EC/DEC electrolytes, the KFSI–DMC electrolyte shows better cycling stability. This result reveals that DMC is a more suitable solvent than DEC and EC/DEC in the KFSI-based electrolyte. These results indicate that the electrolyte solvent can affect the formation of the SEI layer, and thus the electrochemical performance of electrode materials.

Recently, ether-based electrolytes have attracted extensive attention due to the superior electrochemical performance of various electrode materials in PIBs.[63–71] For example, our group reported the superior electrochemical performance of dipotassium terephthalate ($K_2C_8H_4O_4$, K_2TP) in PIBs realized by using a DME-based electrolyte.[63] The K_2TP electrode shows a high reversible capacity (260 mA h g^{-1} at 50 mA g^{-1}), good rate performance (185 mA h g^{-1} at 1000 mA g^{-1}) and superior

cycling stability (capacity retention of 94.6% after 500 cycles). Moreover, we also proposed that the superior electrochemical performance of the K_2TP electrode could be ascribed to the robust and highly K^+-conductive SEI layer formed in the DME-based electrolyte.

Subsequently, Xu and co-workers systematically investigated the reason for the superior electrochemical performance of the anthraquinone-1,5-disulfonic acid sodium salt (AQDS) cathode in the DME-based electrolyte (Fig. 3b).[68] The reaction kinetics of the AQDS electrode in different electrolytes was investigated by the galvanostatic intermittent titration technique and electrochemical impedance spectroscopy measurements. The results reveal that the DME-based electrolyte shows faster reaction kinetics than the EC/DEC-based electrolyte. To better understand the role of the SEI films in the electrochemical performance of the AQDS electrodes, they systematically investigated the SEI in different electrolytes by various characterization methods, including scanning electron microscopy (SEM), transmission electron microscopy (TEM), XPS, and atomic force microscopy (AFM). A thin and stable SEI film formed in the DME electrolyte was observed by SEM and TEM. Compared with the EC/DEC-based electrolyte, more inorganic components were produced in the DME-based electrolyte. Moreover, an inorganic-rich inner layer of SEI film formed in the DME-based electrolyte was demonstrated by Ar^+ ion etching. AFM results show that the AQDS electrode in the DME electrolyte (10.1 GPa) exhibits a higher average Young's modulus than in the EC/DEC electrolyte (3.3 GPa). These results reveal that a dense and stable SEI film formed in the DME-based electrolyte, resulting in favorable performance.

The processes of SEI film formation in the two types of electrolyte were further investigated by theoretical calculations. Fig. 3c shows the HOMO and LUMO energy levels of the solvent and salt species. The LUMO energy level of FSI^- is much lower than that of the DME molecule, indicating that the KFSI will decompose prior to DME (Fig. 3d). In the EC/DEC electrolyte, the decomposition of KFSI, EC and DEC occurred simultaneously because of the highly close LUMO energy levels (Fig. 3e). The fast reaction kinetics and the stable SEI films in the DME electrolyte result in the superior electrochemical performance of AQDS cathodes (capacity retention of 80% after 1000 cycles).

In addition to organic materials, some inorganic materials also show superior electrochemical performance in ether-based electrolytes. Li's group explored the effect of the electrolyte on the electrochemical performance of the TiS_2 cathode for PIBs.[66] They found that the DME-based electrolyte shows better electrochemical performance than the EC/DEC-based electrolyte due to the better kinetics. Subsequently, our group demonstrated that the electrochemical performance of commercial Bi was significantly improved by replacing the conventional ester-based electrolyte with the ether-based electrolyte.[64] Unlike pulverization in the PC-based electrolyte, a 3D porous network of Bi was formed during the charge/discharge processes in the DME-based electrolyte. Density functional theory calculations demonstrate that the strong chemical adsorption of DME molecules on Bi promotes the generation of a 3D porous

structure. The porous structure is beneficial for accommodating the large volume change and facilitating the contact between the electrolyte and the Bi electrode. Therefore, the Bi anode shows a high initial discharge capacity of 496.0 mA h g^{-1} at 0.5 C, superior cycling stability (capacity retention of 86.9% after 300 cycles), and good rate performance (321.9 mA h g^{-1} at 3 C) in 1 M KPF$_6$/DME electrolyte.

Recently, some groups found that the electrochemical behaviors (such as reaction mechanism, capacity, operating potential) of graphitic carbon electrodes can be remarkably changed when ether-based electrolytes were employed.[65,70–73] Pint's group first demonstrated the electrochemical co-intercalation of potassium ion into graphitic carbon electrodes (natural graphite and multi-layered graphene) in ether-based electrolytes (Fig. 4a).[73] The multi-layered graphene foam electrode shows superior cycling stability (capacity retention of 95% after 1000 cycles) and good rate performance (∼80% of the maximum capacity at 10 A g^{-1}). The superior electrochemical performance could be attributed to the weak lattice–host interaction (screening from the co-intercalated solvent) and absence of desolvation to accommodate insertion. Very recently, our group systematically investigated the conditions for reversible K$^+$-solvent co-intercalation by experiments and first-principles calculations.[71] Firstly, we found that the potassium storage behavior of the graphite electrode is closely related

to the solvent species based on experimental results. Then, the density functional theory was used to calculate the solvation energy and desolvation energy of K$^+$–solvent complexes (Fig. 4b and c). The results reveal that the strong solvation of K$^+$ is necessary for K$^+$–solvent co-intercalation. It's worth noting that the K$^+$–solvent co-intercalation behavior in the PC-based electrolyte is not reversible. To further understand the effect of solvents, the LUMO level of the [K–solvent]$^+$ complex ions and the Fermi energy of graphite are calculated by density functional theory. As shown in Fig. 4d, the LUMO level of [K-PC]$^+$ is lower than the Fermi energy of graphite. The result indicated that the reversible K$^+$–solvent co-intercalation requires a higher LUMO level of [K-solvent]$^+$ than the Fermi energy of graphite. Based on the experiments and first-principles calculation results, we proposed that the reversible K$^+$–solvent co-intercalation requires strong solvation of K and high LUMO level of [K-solvent]$^+$ complexes (Fig. 4e). In addition, Pint's group built a PIB system with a Prussian blue cathode, graphite anode and ether-based electrolyte.[65] The full battery shows superior rate performance and cycling stability, which confirms the practicability of ether-based electrolytes. However, ether-based electrolytes generally show relatively poor oxidation stability, which will hinder their compatibility with high-voltage cathode materials. Therefore, finding some effective ways to improve the oxidation stability of ether-based electrolytes is necessary.
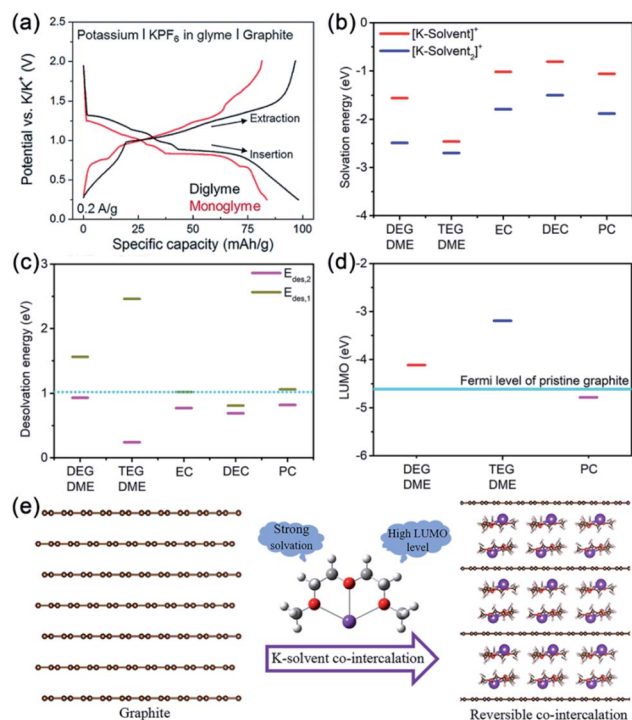

Fig. 4 (a) Charge/discharge curves of graphite electrodes in different electrolytes. Reproduced with permission.[73] Copyright 2016, The Royal Society of Chemistry. (b) Solvation energy of K$^+$−solvent complexes. (c) Desolvation energy of K$^+$−solvent complexes. (d) The LUMO levels of [K-solvent]$^+$ complexes and the Fermi level of graphite. (e) Schematic illustration of the conditions for reversible K$^+$−solvent co-intercalation. (b−e) Reproduced with permission.[71] Copyright 2020, Wiley-VCH.

3.3 Electrolyte concentration optimization

Electrolyte concentration optimization is also considered as an effective strategy to improve the electrochemical performance of electrode materials for PIBs. Wu and co-workers were the pioneers in reporting that the high concentration KFSI–DME electrolyte enables highly reversible potassium plating and stripping due to the formation of a uniform and stable SEI on the surface of potassium metal.[53] In addition, the high-concentration KFSI–DME electrolyte has a wider electrochemical window than the dilute KFSI–DME electrolyte (Fig. 5a). In the high-concentration KFSI–DME electrolyte, the DME molecules tend to donate the oxygen lone pair electrons to K$^+$ (solvation), resulting in lower HOMO energy levels when compared with free DME molecules in the dilute electrolyte (Fig. 5b). The lower HOMO energy level is beneficial for mitigating the oxidative decomposition of the high concentration KFSI–DME electrolyte. Subsequently, Lu's group demonstrated that the cycling performance of perylene-3,4,9,10-tetracarboxylic dianhydride (PTCDA) is significantly improved when using 3 M KFSI DME electrolyte.[74] In the high-concentration electrolyte, the amount of free DME molecules is relatively few, which suppresses the dissolution of the organic electrode. Thus, some other organic materials also show superior cycling stability in the high-concentration electrolyte.[75]

High capacity alloy-type anodes show rapid capacity decay in conventional electrolytes because the large volume change reduces the stability of the SEI layer during the charge/discharge process. Recently, Sun's group investigated the effect of electrolyte concentration on the electrochemical performance (cycling stability and rate performance) of the
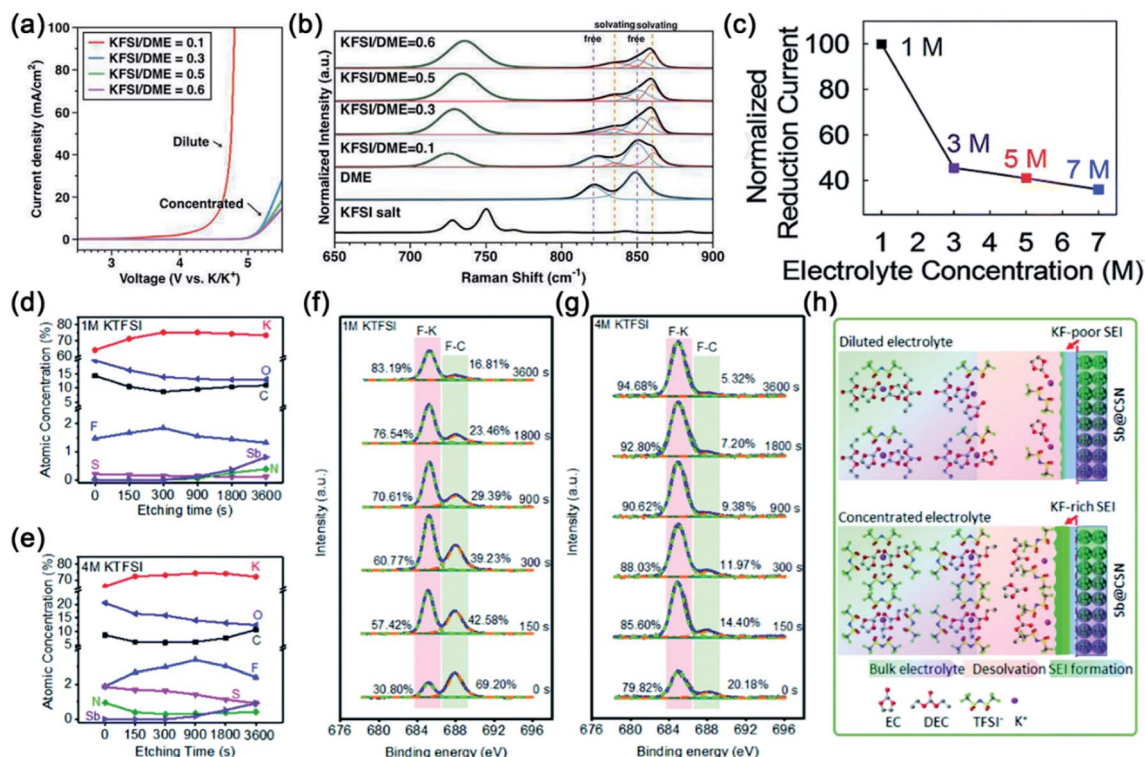
Fig. 5 (a) Electrochemical stability and (b) Raman spectra of the KFSI–DME electrolyte. (a and b) Reproduced with permission.[53] Copyright 2017, American Chemical Society. (c) Normalized reduction current of the electrolyte at different concentrations. Reproduced with permission.[76] Copyright 2019, The Royal Society of Chemistry. (d and e) Atomic percentage concentration of various elements at the etching time in different electrolytes. (f and g) High-resolution F1s XPS spectra of the Sb@CSN electrode in different electrolytes. (h) Schematic illustration of the influence of electrolyte concentration on the formation of the SEI layer. (d–h) Reproduced with permission.[77] Copyright 2019, The Royal Society of Chemistry.

Bi@C anode.[76] The results reveal that electrochemical performance is related to electrolyte concentration. In the 5 M KTFSI/DEGDME electrolyte, the Bi@C anode shows high specific capacity, superior cycling stability, good rate performance and small potential hysteresis. As shown in Fig. 5c, the 5 M electrolyte shows a small reduction current (0.009 mA at 0 V $vs.$ K$^+$/K). The result reveals that the 5 M electrolyte can effectively suppress the side reaction. Subsequently, Wang's group reported that Sb@CSN shows excellent cycling performance in the optimized 4 M KTFSI/EC + DEC electrolyte.[77] To better understand the impact of electrolyte concentration, the chemical compositions of SEI on the surface of Sb@CSN in different electrolytes were investigated by XPS coupled with the Ar$^+$ etching technique (Fig. 5d–g). The results demonstrated that a denser and thinner KF-rich SEI layer formed in 4 M KTFSI electrolyte (Fig. 5h). The KF-rich SEI layer can effectively reduce the side reactions between the electrode materials and electrolyte, and accommodate the volume change of Sb@CSN during charge/discharge processes. Therefore, the Sb@CSN electrode shows outstanding electrochemical performance in 4 M KTFSI electrolyte. In addition, they found that the concentrated electrolyte can mitigate the dissolution issue of KF and decrease the flammability.

The graphite anode shows great potential for PIBs due to its high abundance and low cost. However, the graphite anode shows poor cycling stability when using conventional electrolytes.[78] Recently, Lu's group demonstrated that using concentrated electrolytes (KFSI : EMC, 1 : 2.5, molar ratio) can effectively improve the cycling performance.[79] The graphite anode exhibits negligible capacity fade after cycling for over 2000 cycles due to the formation of a robust inorganic-rich SEI layer on the surface of graphite. Subsequently, Komaba and Wang demonstrated that the high concentration KFSI–DME electrolyte was also beneficial for improving the cycle performance of graphite.[40,80]

HCE can effectively improve the electrochemical performance of electrode materials for PIBs. However, the high viscosity and increased cost of HCE hinder its practical applications.[81] Thus, finding a facile way to overcome these disadvantages is highly essential. Recently, Wu's group prepared a localized high-concentration electrolyte (LHCE) by adding 1,1,2,2-tetrafluoroethyl-2,2,2-trifluoroethyl ether (cost-effective cosolvent) into a concentrated KFSI–DME electrolyte.[82] As shown in Fig. 6a, the local coordination structure of cations was retained in the LHCE. The LHCE shows outstanding oxidation stability (5.3 V $vs.$ K$^+$/K) and high ionic conductivity (13.6 mS cm^{-1}). In addition, the graphite anode in LHCE showed superior cycling stability (reversible capacity of 200 mA h g^{-1} over 300 cycles, Fig. 6b) and rate performance (202 mA h g^{-1} at 4.5 C).
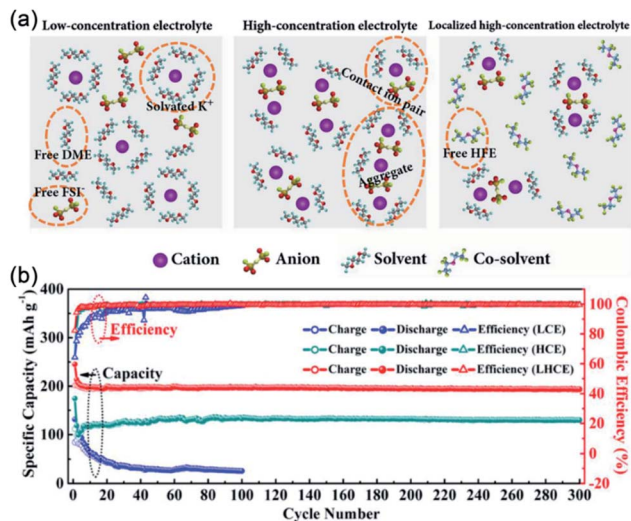
Fig. 6 (a) Schematic illustrations of solution structures of low-concentration electrolyte, HCE and LHCE. (b) Cycling performance of graphite with different electrolytes. (a and b) Reproduced with permission.[82] Copyright 2018, Wiley-VCH.

In addition to these advantages, electrolyte concentration optimization is also an effective strategy to suppress the Al corrosion problem by potassium salts. Komaba's group investigated the effect of concentration of the KFSI-based electrolyte on Al corrosion.[40] After cycling in the 2 mol kg^{-1} KFSI/DME electrolyte, an obvious Al corrosion phenomenon is observed on the Al electrode. However, no morphology change was observed on the Al electrode after cycling in the 7 mol kg^{-1} KFSI/DME electrolyte. The results indicate that the Al corrosion problem by KFSI can be suppressed through electrolyte concentration optimization. In addition, they also found that HCE can improve the electrochemical stability of the electrolyte. Similarly, Passerini et al. also demonstrated that a high concentration of KTFSI is helpful for suppressing the corrosion of Al and enhancing the electrochemical stability of the electrolyte.[83] The superior performance of HCE could be attributed to its limited number of free solvents.

3.4 Introducing electrolyte additives

Introducing electrolyte additives is another effective strategy to improve the electrochemical performance of electrode materials for PIBs. Fluoroethylene carbonate (FEC) has been extensively applied as an electrolyte additive for LIBs and sodium-ion batteries, and it also attracts more and more attention for PIBs.[51,84–89] Nazar's group investigated the effect of FEC additives in an EC/DEC-based electrolyte on the electrochemical performance of the K$_{1.7}$Fe[Fe(CN)$_6$]$_{0.9}$ (KFHCF) cathode.[87] The electrolyte with 5% FEC shows higher coulombic efficiency than the electrolyte without FEC. As shown in Fig. 7a, the KFHCF cathode exhibits superior cycling stability (capacity retention of 60% after 300 cycles) in the electrolyte with 5% FEC. The superior electrochemical performance could be attributed to the introduction of FEC, which effectively suppresses the side reactions of the electrolyte. Subsequently, Wang's group also
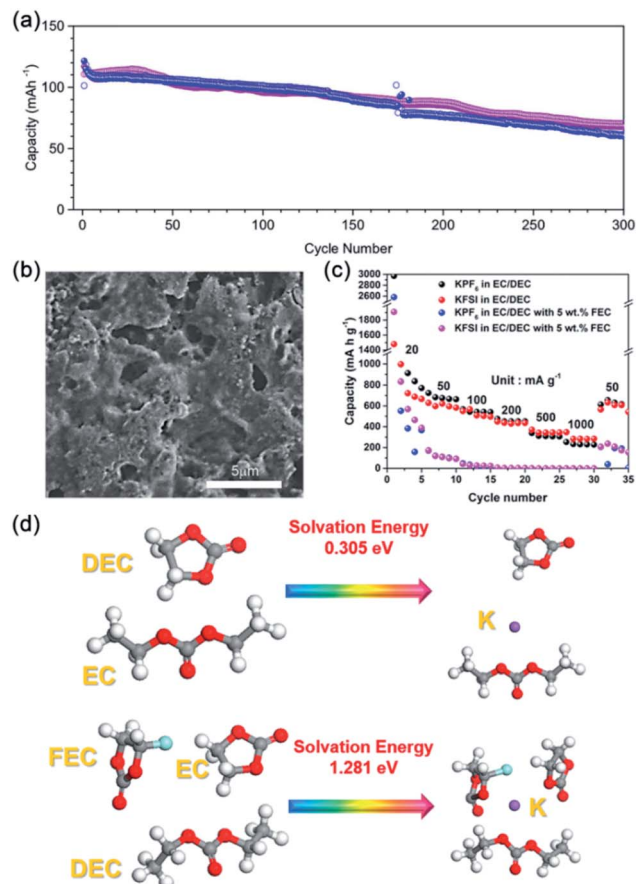

Fig. 7 (a) Cycling performance of KFeHCF electrodes in 0.5 M KPF$_6$ EC/DEC with FEC (note: blue curve, with 2% FEC; pink curve, with 5% FEC). Reproduced with permission.[87] Copyright 2017, American Chemical Society. (b) SEM images of K anodes after cycling in 1 M KPF$_6$ DME with FEC. Reproduced with permission.[88] Copyright 2019, The Royal Society of Chemistry. (c) Rate performance of GeP$_5$ electrodes in four electrolytes. (d) Solvation energies in the electrolyte with and without FEC. (c and d) Reproduced with permission.[57] Copyright 2018, Elsevier.

found that FEC can suppress the formation of dendrites.[88] Obvious K dendrites were formed after 5 cycles in 1 M KPF$_6$ DME electrolyte. After introducing FEC into the electrolyte, the K metal surface remained roughly flat after 5 cycles (Fig. 7b). In addition, Chen et al. found that the electrochemical stability of the electrolyte can be improved by introducing FEC.[89] However, the underlying mechanism toward improving the electrochemical performance by introducing FEC is not clear, and needs further investigation.

According to the above results, FEC is indeed an effective electrolyte additive for PIBs. However, some groups also found the side effect of FEC in PIBs. For example, Yan et al. found that the introduction of FEC into the electrolyte can improve the coulombic efficiency of a pyridinic N-doped porous carbon monolith (PNCM) anode.[90] However, the reversible capacity of the PNCM anode reduced after introducing FEC into the electrolyte. In addition, the graphite anode shows low specific capacity and poor cycle stability after introducing FEC in the
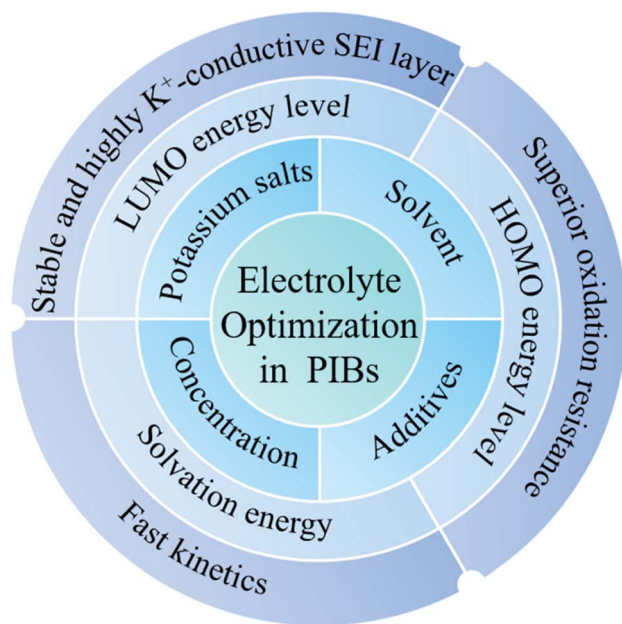
Fig. 8 Summary of strategies for electrolyte optimization in PIBs.

electrolyte.[91] Similarly, Glushenkov *et al.* also reported that the FEC additive led to the deterioration of the cycling stability of the SnS$_2$-reduced graphene oxide anode.[92] Subsequently, Guo's group systematically investigated the effect of FEC additive in PIBs.[57] As shown in Fig. 7c, the GeP$_5$ anode shows inferior electrochemical performance after introducing FEC in the electrolyte. To understand the inferior electrochemical performance of the electrolyte with FEC, the solvation energies were calculated by density functional theory (Fig. 7d). Compared with the solvation energy in the electrolyte without FEC, the electrolyte with FEC shows higher solvation energy (1.281 eV). Therefore, K ion diffusion and desolvation in the electrolyte without FEC occur more easily than in the electrolyte with FEC. Moreover, Fourier transform infrared spectroscopic mapping reveals the formation of inhomogeneous and thick SEI layers in the electrolyte with FEC. Thus, the GeP$_5$ anode shows inferior electrochemical performance in the electrolyte with FEC. Recently, Guo's group also found that the introduction of FEC will increase the electrode polarization.[56] Besides, they proposed that FEC can boost the electrolyte decomposition, thus deteriorating the electrochemical performance of the Sn$_4$P$_3$ electrode. However, the reasons for the different effects of FEC in different battery systems are still unclear and need further investigation.

Apart from the FEC additive, some other electrolyte additives were also applied in PIBs. Madec's group found that vinylene carbonate and FEC as electrolyte additives can improve the coulombic efficiency of the K/Sb half-cell.[93] In addition, KNO$_3$ and KF electrolyte additives were reported by Wang's group.[88] However, the cells using the electrolyte with KNO$_3$ or KF additive show inferior electrochemical performance than that with FEC. Thus, developing novel high-performance electrolyte additives for PIBs is very significant.

4   Conclusions and perspectives

The electrolyte is a key component in PIBs, which significantly affects the electrochemical performance (including cycling stability, rate performance, energy density, *etc.*) of PIBs. In this review, we have summarized the recent progress in electrolyte optimization (including potassium salt optimization, solvent optimization, electrolyte concentration optimization, and introducing electrolyte additives) in PIBs. In general, the reported electrolyte optimization methods can adjust the solvation energy, LUMO energy level, and HOMO energy level, which are beneficial for achieving fast kinetics, stable and highly K$^+$-conductive SEI layer, and superior oxidation resistance, respectively (Fig. 8).

Specifically, the potassium salts mainly influence the components of the SEI layer by adjusting the LUMO energy level. The formed stable and highly K$^+$-conductive SEI layer can improve the rate performance and cycling stability of electrode materials. KFSI is beneficial for the formation of stable SEI layers. However, the corrosion of the Al current collector in the dilute KFSI-based electrolyte inevitably hinders its large-scale application. Therefore, designing novel potassium salts with performance similar to KFSI but free of Al corrosion is very meaningful. The electrolyte solvent is closely related to the solvation energy. Low solvation energy facilitates K$^+$ desolvation and diffusion, and thus improves the kinetics and rate performance. Ether-based electrolytes have attracted more and more attention due to the superior electrochemical performance of various electrode materials in PIBs with ether-based electrolytes. However, the limited electrochemical window of ether-based electrolytes hinders the application of high-voltage cathode materials. Thus, it's urgent to find some novel ether solvent with superior electrochemical stability and effective strategies to improve the oxidation resistance of existing ether-based electrolytes. HCE can reduce the amount of free solvent, which is beneficial for enhancing the oxidation resistance of the electrolyte and promoting the development of high-voltage cathode materials. In addition, HCE can reduce the flammability and Al corrosion, and promote the formation of stable SEI layers. LHCE seems to be an effective strategy to reduce the cost and increase the ionic conductivity of the HCE. Electrolyte additives can affect the solvation energy and the formation of SEI layers but the underlying mechanism is still unclear, and needs to be investigated in the future. All the strategies for electrolyte optimization summarized in this review show huge potential to be extended for other battery systems such as lithium, sodium, and magnesium batteries.

In general, electrode materials with large volume change during the charge/discharge process require a stable SEI layer with fast kinetics and high K$^+$ conductivity to accommodate the volume change, and then realize superior cycling stability and rate performance. Therefore, electrolyte formulations which can promote the formation of the SEI layer with the above properties are highly compatible with the electrode materials featuring large volume change. For the electrode materials which tend to dissolve in the electrolyte, HCE can significantly

improve their cycling performance because of the reduced free solvent. In addition, the electrolyte with low HOMO energy levels shows huge potential for high-voltage PIBs. High-safety PIBs could be realized by using low flammability organic solvents and HCE. Electrolytes with fast kinetics are beneficial for cells to achieve fast charging property.

To meet the demand of high-performance PIBs, further research on organic electrolytes should focus on the following aspects. First, exploring the effects of composition on electrolyte characteristics and the corresponding laws is very meaningful. Second, the SEI and cathode electrolyte interface (CEI) will directly affect the electrochemical performance of electrode materials. Understanding the formation mechanism of SEI and CEI by both *in situ* techniques and density functional theory calculations is necessary with the aim of finding a suitable electrolyte composite to build stable electrode/electrolyte interface layers. Third, PIBs are promising candidates for large-scale energy storage systems, which require some unique properties to satisfy specific applications (such as low temperature and fast charging). Therefore, designing novel electrolytes with low melting point and high ionic conductivity to achieve low-temperature operation and fast charging is very significant. Fourth, it is necessary to develop electrolytes with low flammability and a wide electrochemical stability window to realize high-safety and high-voltage PIBs, respectively. Finally, until now, most of the literature only focused the effect of the electrolyte in half cells with K metal as the reference electrode. To avoid the influence of K metal, the exploration of suitable electrolytes for high-performance PIBs should be carried out based on full cells.

Conflicts of interest

There are no conflicts to declare.

Acknowledgements

References

1 H. Kim, J. C. Kim, M. Bianchini, D.-H. Seo, J. Rodriguez-Garcia and G. Ceder, *Adv. Energy Mater.*, 2018, **8**, 1702384.

2 Q. Zhao, W. Huang, Z. Luo, L. Liu, Y. Lu, Y. Li, L. Li, J. Hu, H. Ma and J. Chen, *Sci. Adv.*, 2018, **4**, eaao1761.

3 Z. Yang, J. Zhang, M. C. Kintner-Meyer, X. Lu, D. Choi, J. P. Lemmon and J. Liu, *Chem. Rev.*, 2011, **111**, 3577–3613.

4 M. Wang and Y. Tang, *Adv. Energy Mater.*, 2018, **8**, 1703320.

5 H. Tan, Y. Feng, X. Rui, Y. Yu and S. Huang, *Small Methods*, 2020, **4**, 1900563.

6 D. Larcher and J. M. Tarascon, *Nat. Chem.*, 2015, **7**, 19–29.

7 K. Song, C. Liu, L. Mi, S. Chou, W. Chen and C. Shen, *Small*, 2019, DOI: 10.1002/smll.201903194.

8 D. M. Davies, M. G. Verde, O. Mnyshenko, Y. R. Chen, R. Rajeev, Y. S. Meng and G. Elliott, *Nat. Energy*, 2019, **4**, 42–50.

9 B. Dunn, H. Kamath and J.-M. Tarascon, *Science*, 2011, **334**, 928–935.

10 C. Zhong, B. Liu, J. Ding, X. Liu, Y. Zhong, Y. Li, C. Sun, X. Han, Y. Deng, N. Zhao and W. Hu, *Nat. Energy*, 2020, **5**, 440–449.

11 Y. Lu, Q. Zhang, L. Li, Z. Niu and J. Chen, *Chem*, 2018, **4**, 2786–2813.

12 Z. Lin, Q. Xia, W. Wang, W. Li and S. Chou, *InfoMat*, 2019, **1**, 376–389.

13 J. Wu, Y. Cao, H. Zhao, J. Mao and Z. Guo, *Carbon Energy*, 2019, **1**, 57–76.

14 L. Li, Y. Lu, Q. Zhang, S. Zhao, Z. Hu and S. L. Chou, *Small*, 2019, DOI: 10.1002/smll.201902767.

15 J. Chen, D. H. C. Chua and P. S. Lee, *Small Methods*, 2020, **4**, 1900648.

16 T. Hosaka, K. Kubota, A. S. Hameed and S. Komaba, *Chem. Rev.*, 2020, **120**, 6358–6466.

17 Z. Liu, J. Wang, X. Jia, W. Li, Q. Zhang, L. Fan, H. Ding, H. Yang, X. Yu, X. Li and B. Lu, *ACS Nano*, 2019, **13**, 10631–10642.

18 Y. Liu, Z. Tai, J. Zhang, W. K. Pang, Q. Zhang, H. Feng, K. Konstantinov, Z. Guo and H. K. Liu, *Nat. Commun.*, 2018, **9**, 3645.

19 J. Zhou, Y. Liu, S. Zhang, T. Zhou and Z. Guo, *InfoMat*, 2020, **2**, 437–465.

20 J.-Y. Hwang, S.-T. Myung and Y.-K. Sun, *Adv. Funct. Mater.*, 2018, **28**, 1802938.

21 M. Okoshi, Y. Yamada, S. Komaba, A. Yamada and H. Nakai, *J. Electrochem. Soc.*, 2017, **164**, A54–A60.

22 J. C. Pramudita, D. Sehrawat, D. Goonetilleke and N. Sharma, *Adv. Energy Mater.*, 2017, **7**, 1602911.

23 M. Sha, L. Liu, H. Zhao and Y. Lei, *Carbon Energy*, 2020, **2**, 350–369.

24 K. Lei, Z. Zhu, Z. Yin, P. Yan, F. Li and J. Chen, *Chem*, 2019, **5**, 3220–3231.

25 M. Ye, J.-Y. Hwang and Y.-K. Sun, *ACS Nano*, 2019, **13**, 9306–9314.

26 H. Gao, L. Xue, S. Xin and J. B. Goodenough, *Angew. Chem., Int. Ed.*, 2018, **57**, 5449–5453.

27 H. Kim, D.-H. Seo, M. Bianchini, R. J. Clément, H. Kim, J. C. Kim, Y. Tian, T. Shi, W.-S. Yoon and G. Ceder, *Adv. Energy Mater.*, 2018, **8**, 1801591.

28 K. Share, A. P. Cohn, R. Carter, B. Rogers and C. L. Pint, *ACS Nano*, 2016, **10**, 9738–9744.

29 Q. Xue, D. Li, Y. Huang, X. Zhang, Y. Ye, E. Fan, L. Li, F. Wu and R. Chen, *J. Mater. Chem. A*, 2018, **6**, 12559–12564.

30 Y. An, Y. Tian, L. Ci, S. Xiong, J. Feng and Y. Qian, *ACS Nano*, 2018, **12**, 12932–12940.

31 Z. Tong, R. Yang, S. Wu, D. Shen, T. Jiao, K. Zhang, W. Zhang and C.-S. Lee, *Small*, 2019, **15**, 1901272.

32 Y. Lu, L. Li, Q. Zhang, Z. Niu and J. Chen, *Joule*, 2018, **2**, 1747–1770.

33 L. Fan, S. Chen, R. Ma, J. Wang, L. Wang, Q. Zhang, E. Zhang, Z. Liu and B. Lu, *Small*, 2018, **14**, 1801806.

34 H. Che, S. Chen, Y. Xie, H. Wang, K. Amine, X.-Z. Liao and Z.-F. Ma, *Energy Environ. Sci.*, 2017, **10**, 1075–1101.

35 Q. Liu, Z. Hu, Y. Liang, L. Li, C. Zou, H. Jin, S. Wang, H. Lu, Q. Gu, S. Chou, Y. Liu and S.-X. Dou, *Angew. Chem., Int. Ed.*, 2020, **59**, 5159–5164.

36 L. Jiang, Y. Lu, C. Zhao, L. Liu, J. Zhang, Q. Zhang, X. Shen, J. Zhao, X. Yu, H. Li, X. Huang, L. Chen and Y.-S. Hu, *Nat. Energy*, 2019, **4**, 495–503.

37 K. Yoshii, T. Masese, M. Kato, K. Kubota, H. Senoh and M. Shikano, *ChemElectroChem*, 2019, **6**, 3901–3910.

38 W. Zhang, Y. Liu and Z. Guo, *Sci. Adv.*, 2019, **5**, eaav7412.

39 K. Xu, *Chem. Rev.*, 2004, **104**, 4303–4418.

40 T. Hosaka, K. Kubota, H. Kojima and S. Komaba, *Chem. Commun.*, 2018, **54**, 8387–8390.

41 Q. Zhang, J. Mao, W. K. Pang, T. Zheng, V. Sencadas, Y. Chen, Y. Liu and Z. Guo, *Adv. Energy Mater.*, 2018, **8**, 1703288.

42 H. Lin, M. Li, X. Yang, D. Yu, Y. Zeng, C. Wang, G. Chen and F. Du, *Adv. Energy Mater.*, 2019, **9**, 1900323.

43 Z. Wang, K. Dong, D. Wang, S. Luo, Y. Liu, Q. Wang, Y. Zhang, A. Hao, C. Shi and N. Zhao, *J. Mater. Chem. A*, 2019, **7**, 14309–14318.

44 Q. Tan, P. Li, K. Han, Z. Liu, Y. Li, W. Zhao, D. He, F. An, M. Qin and X. Qu, *J. Mater. Chem. A*, 2019, **7**, 744–754.

45 J.-W. Choi, J.-K. Kim, G. Cheruvally, J.-H. Ahn, H.-J. Ahn and K.-W. Kim, *Electrochim. Acta*, 2007, **52**, 2075–2082.

46 J. Xie, X. Li, H. Lai, Z. Zhao, J. Li, W. Zhang, W. Xie, Y. Liu and W. Mai, *Angew. Chem., Int. Ed.*, 2019, **58**, 14740–14747.

47 Q. Zhao, J. Wang, Y. Lu, Y. Li, G. Liang and J. Chen, *Angew. Chem., Int. Ed.*, 2016, **55**, 12528–12532.

48 X. Tang, D. Zhou, P. Li, X. Guo, B. Sun, H. Liu, K. Yan, Y. Gogotsi and G. Wang, *Adv. Mater.*, 2020, **32**, 1906739.

49 J. Li, N. Zhuang, J. Xie, X. Li, W. Zhuo, H. Wang, J. B. Na, X. Li, Y. Yamauchi and W. Mai, *Adv. Energy Mater.*, 2020, **10**, 1903455.

50 Z. Tong, S. Tian, H. Wang, D. Shen, R. Yang and C.-S. Lee, *Adv. Funct. Mater.*, 2020, **30**, 1907656.

51 A. S. Hameed, A. Katogi, K. Kubota and S. Komaba, *Adv. Energy Mater.*, 2019, **9**, 1902528.

52 H. Wang, H. Wang, S. Chen, B. Zhang, G. Yang, P. Gao, J. Liu, X. Fan, Y. Huang, J. Lin and Z. Shen, *ACS Appl. Energy Mater.*, 2019, **2**, 7942–7951.

53 N. Xiao, W. D. McCulloch and Y. Wu, *J. Am. Chem. Soc.*, 2017, **139**, 9475–9478.

54 H. Wang, D. Yu, X. Wang, Z. Niu, M. Chen, L. Cheng, W. Zhou and L. Guo, *Angew. Chem., Int. Ed.*, 2019, **58**, 16451–16455.

55 W. Luo, F. Li, W. Zhang, K. Han, J.-J. Gaumet, H.-E. Schaefer and L. Mai, *Nano Res.*, 2019, **12**, 1025–1031.

56 W. Zhang, W. K. Pang, V. Sencadas and Z. Guo, *Joule*, 2018, **2**, 1534–1547.

57 W. Zhang, Z. Wu, J. Zhang, G. Liu, N.-H. Yang, R.-S. Liu, W. K. Pang, W. Li and Z. Guo, *Nano Energy*, 2018, **53**, 967–974.

58 L. Deng, Y. Zhang, R. Wang, M. Feng, X. Niu, L. Tan and Y. Zhu, *ACS Appl. Mater. Interfaces*, 2019, **11**, 22449–22456.

59 J. Zhao, X. Zou, Y. Zhu, Y. Xu and C. Wang, *Adv. Funct. Mater.*, 2016, **26**, 8103–8110.

60 J. Dong, Y. Lei, D. Han, H. Wang, D. Zhai, B. Li and F. Kang, *Chem. Commun.*, 2019, **55**, 12555–12558.

61 L. Liu, Z. Lin, J.-Y. Chane-Ching, H. Shao, P.-L. Taberna and P. Simon, *Energy Storage Mater.*, 2019, **19**, 306–313.

62 Z. Wu, G. Liang, W. K. Pang, T. Zhou, Z. Cheng, W. Zhang, Y. Liu, B. Johannessen and Z. Guo, *Adv. Mater.*, 2020, **32**, 1905632.

63 K. Lei, F. Li, C. Mu, J. Wang, Q. Zhao, C. Chen and J. Chen, *Energy Environ. Sci.*, 2017, **10**, 552–557.

64 K. Lei, C. Wang, L. Liu, Y. Luo, C. Mu, F. Li and J. Chen, *Angew. Chem., Int. Ed.*, 2018, **57**, 4687–4691.

65 K. Moyer, J. Donohue, N. Ramanna, A. P. Cohn, N. Muralidharan, J. Eaves and C. L. Pint, *Nanoscale*, 2018, **10**, 13335–13342.

66 L. Wang, J. Zou, S. Chen, G. Zhou, J. Bai, P. Gao, Y. Wang, X. Yu, J. Li, Y.-S. Hu and H. Li, *Energy Storage Mater.*, 2018, **12**, 216–222.

67 Y. Bai, W. Fu, W. Chen, Z. Chen, X. Pan, X. Lv, J. Wu and X. Pan, *J. Mater. Chem. A*, 2019, **7**, 24454–24461.

68 B. Li, J. Zhao, Z. Zhang, C. Zhao, P. Sun, P. Bai, J. Yang, Z. Zhou and Y. Xu, *Adv. Funct. Mater.*, 2019, **29**, 1807137.

69 Q. Tan, W. Zhao, K. Han, P. Li, W. Wang, D. He, Z. Liu, Q. Yu, M. Qin and X. Qu, *J. Mater. Chem. A*, 2019, **7**, 15673–15682.

70 L. Wang, J. Yang, J. Li, T. Chen, S. Chen, Z. Wu, J. Qiu, B. Wang, P. Gao, X. Niu and H. Li, *J. Power Sources*, 2019, **409**, 24–30.

71 L. Li, L. Liu, Z. Hu, Y. Lu, Q. Liu, S. Jin, Q. Zhang, S. Zhao and S. L. Chou, *Angew. Chem., Int. Ed.*, 2020, **59**, 12917–12924.

72 H. Kim, G. Yoon, K. Lim and K. Kang, *Chem. Commun.*, 2016, **52**, 12618–12621.

73 A. P. Cohn, N. Muralidharan, R. Carter, K. Share, L. Oakes and C. L. Pint, *J. Mater. Chem. A*, 2016, **4**, 14954–14959.

74 L. Fan, R. Ma, J. Wang, H. Yang and B. Lu, *Adv. Mater.*, 2018, **30**, 1805486.

75 M. Xiong, W. Tang, B. Cao, C. Yang and C. Fan, *J. Mater. Chem. A*, 2019, **7**, 20127–20131.

76 R. Zhang, J. Bao, Y. Wang and C.-F. Sun, *Chem. Sci.*, 2018, **9**, 6193–6198.

77 J. Zheng, Y. Yang, X. Fan, G. Ji, X. Ji, H. Wang, S. Hou, M. R. Zachariah and C. Wang, *Energy Environ. Sci.*, 2019, **12**, 615–623.

78 Z. Jian, W. Luo and X. Ji, *J. Am. Chem. Soc.*, 2015, **137**, 11566–11569.

79 L. Fan, R. Ma, Q. Zhang, X. Jia and B. Lu, *Angew. Chem., Int. Ed.*, 2019, **58**, 10500–10505.

80 X. Niu, L. Li, J. Qiu, J. Yang, J. Huang, Z. Wu, J. Zou, C. Jiang, J. Gao and L. Wang, *Solid State Ionics*, 2019, **341**, 115050.

81 Y. Yamada, J. Wang, S. Ko, E. Watanabe and A. Yamada, *Nat. Energy*, 2019, **4**, 269–280.

82 L. Qin, N. Xiao, J. Zheng, Y. Lei, D. Zhai and Y. Wu, *Adv. Energy Mater.*, 2019, **9**, 1902618.

83 X. Liu, G. A. Elia, X. Gao, B. Qin, H. Zhang and S. Passerini, *Batteries Supercaps*, 2020, **3**, 261–267.

84 A. Darwiche, C. Marino, M. T. Sougrati, B. Fraisse, L. Stievano and L. Monconduit, *J. Am. Chem. Soc.*, 2012, **134**, 20805–20811.

85 X. Bian, Y. Dong, D. Zhao, X. Ma, M. Qiu, J. Xu, L. Jiao, F. Cheng and N. Zhang, *ACS Appl. Mater. Interfaces*, 2020, **12**, 3554–3562.

86 X. Jiang, T. Zhang, L. Yang, G. Li and J. Y. Lee, *ChemElectroChem*, 2017, **4**, 2237–2242.

87 G. He and L. F. Nazar, *ACS Energy Lett.*, 2017, **2**, 1122–1127.

88 M. Tang, Y. Wu, Y. Chen, C. Jiang, S. Zhu, S. Zhuo and C. Wang, *J. Mater. Chem. A*, 2019, **7**, 486–492.

89 J. Liao, Q. Hu, Y. Yu, H. Wang, Z. Tang, Z. Wen and C. Chen, *J. Mater. Chem. A*, 2017, **5**, 19017–19024.

90 Y. Xie, Y. Chen, L. Liu, P. Tao, M. Fan, N. Xu, X. Shen and C. Yan, *Adv. Mater.*, 2017, **29**, 1702268.

91 X. Bie, K. Kubota, T. Hosaka, K. Chihara and S. Komaba, *J. Mater. Chem. A*, 2017, **5**, 4325–4330.

92 V. Lakshmi, Y. Chen, A. A. Mikhaylov, A. G. Medvedev, I. Sultana, M. M. Rahman, O. Lev, P. V. Prikhodchenko and A. M. Glushenkov, *Chem. Commun.*, 2017, **53**, 8272–8275.

93 L. Madec, V. Gabaudan, G. Gachot, L. Stievano, L. Monconduit and H. Martinez, *ACS Appl. Mater. Interfaces*, 2018, **10**, 34116–34122.